1 Structural Properties

1.1 IONICITY

1.1.1 Definition

All tetrahedrally coordinated $A^N B^{8-N}$ semiconductors can be treated within the framework of a simple model. The success of this approach requires a careful choice of parameters entering in the model. The most important of these is the ionicity of the bond [1.1].

The ionicity of a bond can be defined as the fraction f_i^α of ionic or heteropolar character in the bond compared with the fraction f_h^α of covalent or homopolar character. By definition, these fractions satisfy the relation

$$f_i^\alpha + f_h^\alpha = 1 \tag{1.1}$$

In an elemental semiconductor such as Si, we must have $f_h^\alpha = 1$ and $f_i^\alpha = 0$. In contrast, we shall find that some alkali halides (NaCl, KCl, etc.) are more than 90% ionic.

Properties of Group-IV, III–V and II–VI Semiconductors Sadao Adachi
 ISBN: 0-470-09032-4

(a) Phillips ionicity

Phillips studied the connection between the chemical bonding properties of the $A^N B^{8-N}$ family of crystals and their electronic energy-band structures [1.1]. His concept evolves from a molecular picture in terms of bonding and antibonding states separated by an energy gap E_g. His ionicity scale f_i is defined in terms of average quantities such as the homopolar E_h and heteropolar parts C of the complex energy gap E_g associated with the A–B bond in the crystal

$$E_g = E_h + iC \tag{1.2}$$

Ionicity is then introduced via the relation

$$f_i = \frac{C^2}{E_g^2} = \frac{C^2}{E_h^2 + C^2} \tag{1.3}$$

Some numerical examples of E_g (f_i) are: $E_g = 4.70 + i0$ ($f_i = 0$) for Si; $E_g = 4.32 + i2.90$ ($f_i = 0.310$) for GaAs; $E_g = 4.29 + i5.60$ ($f_i = 0.630$) for ZnSe, where E_g are in eV.

(b) Pauling ionicity

Pauling based his definition of ionicity scale f_i^P not on the total energy of the bond, but on empirical heats of formation [1.2]. Denote the power of an atom A to attract electrons to itself by a dimensionless number called its electronegativity X_A. The Coulomb interaction between the ionic charge left behind and the valence charge transferred is proportional to $(X_A - X_B)^2$, and this is the origin of the extra ionic energy (i.e., f_i^P). By definition f_i^P never exceeds one, and as $X_A - X_B$ becomes large f_i^P tends to one. Moreover, the ionicity of an A–B bond should be the same as ionicity of a B–A bond. Pauling then defined ionicity of a single bond

$$f_i^P = 1 - \exp\left(-\frac{(X_A - X_B)^2}{4}\right) \tag{1.4}$$

(c) Harrison ionicity

In Harrison's model [1.3], the ionicity parameter f_i^H can be given in terms of two of the parameters of the electronic structure, by

$$f_i^H = \frac{V_3}{\sqrt{V_2^2 + V_3^2}} \tag{1.5}$$

Here, V_2 is half the splitting between bonding and antibonding states; V_3 is half the energy change in transferring an electron from anion to cation. This parameter f_i^H can be defined as the excess number of electrons placed on the anion from each bond, called the polarity. Thus, each anion in a tetrahedral structure contains a charge of $Z^* = 4f_i^H - \Delta Z$,

Table 1.1 Phillips (f_i), Pauling (f_i^P) and Harrison ionicities (f_i^H) for a number of group-IV, III–V and II–VI semiconductors

System	Material	f_i	f_i^P	f_i^H	System	Material	f_i	f_i^P	f_i^H
IV	Diamond	0	0	0	II–VI	MgO	0.841	0.88	
	Si	0	0	0		MgS	0.786		
	Ge	0	0	0		MgSe	0.790		
	Sn	0	0	0		MgTe	0.554		
	SiC	0.177	0.11	0.35		ZnO	0.616	0.80	0.69
						ZnS	0.623	0.59	0.69
III–V	BN	0.221	0.42	0.43		ZnSe	0.630	0.57	0.70
	BP	0.032				ZnTe	0.609	0.53	0.68
	BAs	0.044				CdS	0.685	0.59	0.74
	AlN	0.449	0.56	0.57		CdSe	0.699	0.58	0.74
	AlP	0.307	0.25	0.47		CdTe	0.717	0.52	0.76
	AlAs	0.274	0.27	0.44		HgS	0.790		
	AlSb	0.250	0.26	0.56		HgSe	0.680		
	GaN	0.500	0.55	0.61		HgTe	0.650		0.78
	GaP	0.327	0.27	0.48					
	GaAs	0.310	0.26	0.47					
	GaSb	0.261	0.26	0.43					
	InN	0.578							
	InP	0.421	0.26	0.55					
	InAs	0.357	0.26	0.51					
	InSb	0.321	0.25	0.48					

where ΔZ is the difference in valence from 4 ($\Delta Z = 1$ for nitrogen, 2 for oxygen, etc.). Similarly, then, each bond provides an electronic dipole moment of $\boldsymbol{P} = \gamma f_i^H$ $(-e\boldsymbol{d})$, where $\boldsymbol{d}$ is vector distance from cation to anion and γ is a scale parameter to take into account local fields and charge symmetries; a value of $\sqrt{2}$ gave a good fit to experiment.

1.1.2 Ionicity value

Table 1.1 summarizes the values of Phillips (f_i) [1.1], Pauling (f_i^P) [1.2] and Harrison ionicities (f_i^H) [1.3] for a number of group-IV, III–V and II–VI semiconductors. We also show in Figure 1.1 Phillips ionicity f_i versus (a) Pauling (f_i^P) and (b) Harrison ionicities (f_i^H) for these semiconductors.

1.2 ELEMENTAL ISOTOPIC ABUNDANCE AND MOLECULAR WEIGHT

1.2.1 Elemental isotopic abundance

There are a great many semiconductor materials. We list in Table 1.2 the elements which form at least one tetrahedrally coordinated $A^N B^{8-N}$ semiconductor, together with their

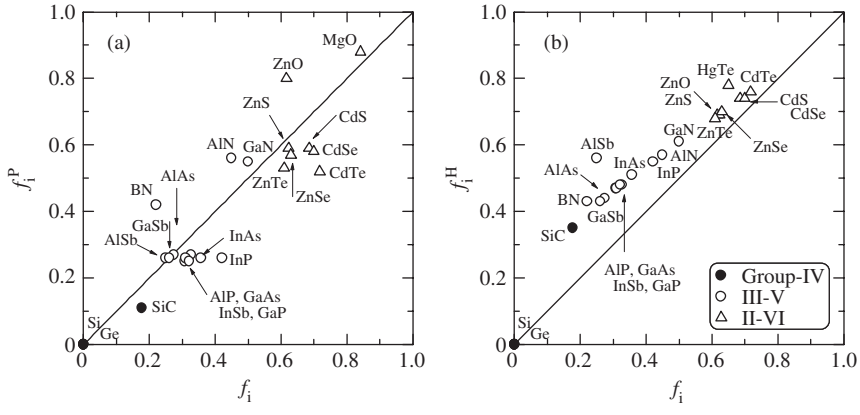

Figure 1.1 Phillips ionicity f_i versus (a) Pauling (f_i^P) and (b) Harrison ionicities (f_i^H) for some group-IV, III–V and II–VI semiconductors. The solid lines in (a) and (b) indicate the relations of $f_i = f_i^P$ and $f_i = f_i^H$, respectively

natural isotopic abundance in percent [1.4]. Table 1.3 also lists the standard atomic weight for some group IV, III, V, II and VI elements [1.4].

1.2.2 Molecular weight

The molecular weight M for an $A^N B^{8-N}$ semiconductor ($N \neq 4$) can be simply given by the sum of the atomic weights of atoms A and B. For an elemental semiconductor ($N = 4$), it is given by the atomic weight of the element atom A = B. Tables 1.4 and 1.5 list the values of M for a number of group-IV, III–V and II–VI semiconductors with cubic and hexagonal (rhombohedral) structures, respectively.

1.3 CRYSTAL STRUCTURE AND SPACE GROUP

1.3.1 Crystal structure

(a) Diamond, zinc-blende and wurtzite structures

The atoms of certain elements are held together in the solid by strongly covalent bonds at tetrahedral angles of 109.5°. Each atom has four nearest neighbors and twelve next nearest neighbors, which is a consequence of each atom sharing one of its outer electrons with each of four neighbors. The typical structure so formed is that of *diamond*, as shown in Figure 1.2(a). The space lattice is face-centered cubic with pairs of atoms at (0, 0, 0) and (1/4, 1/4, 1/4) forming a pattern unit.

The atomic orbitals that are used to form hybridized bonding orbitals are usually not the same ones that are occupied in the ground state of the atom. For example, in silicon the ground valence configuration of the atom is $3s^2 3p^2$, whereas the hybridized configuration appropriate for the diamond-type crystal structure is $3s^1 3p^3$ (tetrahedral coordination).

Table 1.2 Natural isotopic abundance in percent for some group IV, III, V, II and VI elements

Group	Isotope	Natural abundance (%)	Group	Isotope	Natural abundance (%)
IV	^{12}C	98.90	IV	^{112}Sn	0.97
	^{13}C	1.10		^{114}Sn	0.65
	^{28}Si	92.23		^{115}Sn	0.34
	^{29}Si	4.67		^{116}Sn	14.53
	^{30}Si	3.10		^{117}Sn	7.68
	^{70}Ge	21.23		^{118}Sn	24.23
	^{72}Ge	27.66		^{119}Sn	8.59
	^{73}Ge	7.73		^{120}Sn	32.59
	^{74}Ge	35.94		^{122}Sn	4.63
	^{76}Ge	7.44		^{124}Sn	5.79
III	^{10}B	19.9	V	^{14}N	99.634
	^{11}B	80.1		^{15}N	0.366
	^{27}Al	100		^{31}P	100
	^{69}Ga	60.108		^{75}As	100
	^{71}Ga	39.892		^{121}Sb	57.36
	^{113}In	4.3		^{123}Sb	42.64
	^{115}In	95.7			
II	^{24}Mg	78.99	VI	^{16}O	99.762
	^{25}Mg	10.00		^{17}O	0.038
	^{26}Mg	11.01		^{32}S	95.02
	^{64}Zn	48.6		^{33}S	0.75
	^{66}Zn	27.9		^{34}S	4.21
	^{67}Zn	4.1		^{36}S	0.02
	^{68}Zn	18.8		^{74}Se	0.89
	^{70}Zn	0.6		^{76}Se	9.36
	^{106}Cd	1.25		^{77}Se	7.63
	^{108}Cd	0.89		^{78}Se	23.78
	^{110}Cd	12.49		^{80}Se	49.61
	^{111}Cd	12.80		^{82}Se	8.73
	^{112}Cd	24.13		^{120}Te	0.096
	^{113}Cd	12.22		^{122}Te	2.603
	^{114}Cd	28.73		^{123}Te	0.908
	^{116}Cd	7.49		^{124}Te	4.816
	^{196}Hg	0.15		^{125}Te	7.139
	^{198}Hg	9.97		^{126}Te	18.95
	^{199}Hg	16.87		^{128}Te	31.69
	^{200}Hg	23.10		^{130}Te	33.80
	^{201}Hg	13.18			
	^{202}Hg	29.86			
	^{204}Hg	6.87			

Table 1.3 Standard atomic weight for some group IV, III, V, II and VI elements. Numbers in parentheses give the uncertainty in the last digit of the stated values

Group	Symbol	Atomic weight	Group	Symbol	Atomic weight
IV	C	12.0107(8)			
	Si	28.0855(3)			
	Ge	72.61(2)			
	Sn	118.710(7)			
III	B	10.811(7)	V	N	14.00674(7)
	Al	26.981538(2)		P	30.973761(2)
	Ga	69.723(1)		As	74.921560(2)
	In	114.818(3)		Sb	121.760(1)
II	Mg	24.3050(6)	VI	O	15.9994(3)
	Zn	65.39(2)		S	32.066(6)
	Cd	112.411(8)		Se	78.96(3)
	Hg	200.59(2)		Te	127.60(3)

The diamond cubic lattice is a consequence of the carbon valency of four. We can expect to find the same structure in compounds where one atom has more than four electrons and the other the same number less than four, so that a total of four valency electrons to each atom is maintained. If the compound is of the form of AB, this structure can be produced in two ways. The first is the cubic, *zinc-blende* structure as shown in Figure 1.2(b), with four A (Ga) and four B (As) atoms per conventional unit cell.

The second method by which a structure is formed where each atom of one kind is surrounded by four of another is shown in Figure 1.2(c). This is the hexagonal CdS (w-CdS or β-CdS) or *wurtzite* lattice, which differs only from the zinc-blende structure in the stacking sequence of the sulfur layers. Ideally, the wurtzite structure has the axial ratio $c/a = (8/3)^{1/2} = 1.633$ (hexagonal close-packed structure). Most III–V semiconductors crystallize in the zinc-blende structure, however, many II–VI and some III–V semiconductors crystallize in the wurtzite structure.

In III–V compounds, group III atoms have three electrons with an s^2p^1-configuration outside a core of closed shells and group V atoms five electrons in a s^2p^3-configuration. The III and V atoms have, therefore, an average of four valence electrons per atom available for bonding. We might then expect that the covalent bonds are formed between tetrahedral s^1p^3-hybrid orbitals, e.g., for GaAs:

$$\mathrm{Ga}(4s^24p^1) + \mathrm{As}(4s^24p^3) \rightarrow \mathrm{Ga}(4s^14p^3)^- + \mathrm{As}(4s^14p^3)^+ \tag{1.6}$$

For such a covalent bonding each V atom donates an electron to a III atom, so that V^+ and III^- ions are formed, each with four valence electrons.

An ionic bond is due to Coulomb attraction between the excess positive and negative charges on ions formed by transfer of electrons from the metallic to the nonmetallic atom in the scheme:

$$\mathrm{Ga}(4s^24p^1) + \mathrm{As}(4s^24p^3) \rightarrow \mathrm{Ga}(4s^04p^0)^{+3} + \mathrm{As}(4s^24p^6)^{-3} \tag{1.7}$$

Table 1.4 Molecular weight M, lattice constant a and crystal density g for a number of cubic group-IV, III–V and II–VI semiconductors at 300 K

System	Material	M (amu)	a (Å)	g (g/cm^3)
IV	Diamond	12.0107	3.5670	3.5156
	Si	28.0855	5.4310	2.3291
	Ge	72.61	5.6579	5.3256
	α-Sn	118.710	6.4892	5.7710
	3C-SiC	40.0962	4.3596	3.2142
III–V	c-BN	24.818	3.6155	3.4880
	BP	41.785	4.5383	2.9693
	BAs	85.733	4.777	5.224
	c-AlN	40.98828	4.38	3.24
	AlP	57.955299	5.4635	2.3604
	AlAs	101.903098	5.66139	3.73016
	AlSb	148.742	6.1355	4.2775
	β-GaN	83.730	4.52	6.02
	GaP	100.696	5.4508	4.1299
	GaAs	144.645	5.65330	5.31749
	GaSb	191.483	6.09593	5.61461
	InP	145.792	5.8690	4.7902
	InAs	189.740	6.0583	5.6678
	InSb	236.578	6.47937	5.77677
II–VI	MgO	40.3044	4.203	3.606
	β-MgS	56.371	5.62	2.11
	β-MgSe	103.27	5.91	3.32
	β-MgTe	151.91	6.42	3.81
	β-ZnS	97.46	5.4102	4.0879
	ZnSe	144.35	5.6692	5.2621
	ZnTe	192.99	6.009	5.908
	c-CdS	144.477	5.825	4.855
	c-CdSe	191.37	6.077	5.664
	CdTe	240.01	6.481	5.856
	β-HgS	232.66	5.8514	7.7135
	HgSe	279.55	6.084	8.245
	HgTe	328.19	6.4603	8.0849

The bonds in most III–V or II–VI semiconductors are not adequately described by any of these extreme types, but have characteristics intermediate to those usually associated with the terms covalent (Equation (1.6)) and ionic (Equation (1.7)).

(b) Hexagonal and rhombohedral structures

It is well known that silicon carbide (SiC) is a semiconductor crystallizing in a large number of polytypes [1.5]. The various types of SiC differ one from another only by the

Table 1.5 Molecular weight M, lattice constants a and c and crystal density g for a number of hexagonal and rhombohedral group-IV, III–V and II–VI semiconductors at 300 K

System	Material	M (amu)	Lattice constant (Å)		g (g/cm^3)
			a	c	
IV	6H-SiC	40.0962	3.0806	15.1173	3.2153
	15R-SiC	40.0962	3.079 ($\alpha = 13^\circ 54.5'$)	37.78	
III–V	h-BN	24.818	2.5040	6.6612	2.2787
	w-AlN	40.98828	3.112	4.982	3.258
	α-GaN	83.730	3.1896	5.1855	6.0865
	InN	128.825	3.548	5.760	6.813
II–VI	ZnO	81.39	3.2495	5.2069	5.6768
	α-ZnS	97.46	3.8226	6.2605	4.0855
	w-CdS	144.477	4.1367	6.7161	4.8208
	w-CdSe	191.37	4.2999	7.0109	5.6615

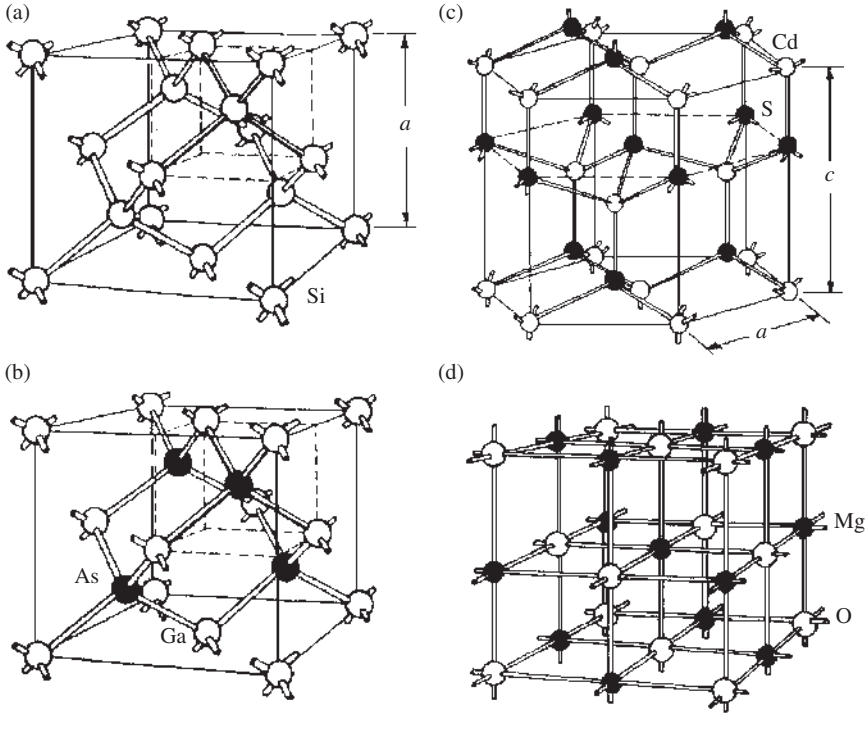

Figure 1.2 Some important crystal lattice structures. (a) diamond lattice (Si); (b) zinc-blende lattice (GaAs); (c) wurtzite lattice (w-CdS); and (d) rocksalt lattice (MgO)

order in which successive planes of Si (or C) atoms are stacked along the *c* axis; one polytype is cubic (3C-SiC) while the remainder, including two of the more frequently occurring forms, 6H and 15R, possess uniaxial symmetry. Note that in the polytype name, the integer refers to the number of Si (C) layers in the unit cell, and C, H and R indicate cubic, hexagonal and rhombohedral (trigonal) symmetry, respectively. Of all the polytypes, 6H is by far the most commonly occurring modification in commercial SiC. The next most common types are 15R and 4H, respectively. Silicon carbide can also crystallize in the wurtzite structure (2H-SiC).

Figure 1.3 shows the stacking sequences in 3C-SiC, 2H-SiC and 6H-SiC [1.6]. In the zinc-blende (3C) structure, the sequence involves three layers which are repeated periodically (ABC ABC . . .). All the Si–C bond lengths are the same, and the angles are exactly tetrahedral (109.5°). In the wurtzite (2H) structure, only two layers are repeated (AB AB . . .). The Si–C bond length along the stacking direction is not equal to that which is approximately perpendicular to it, and the angles are not exactly tetrahedral. In the 6H polytype, the basic sequence involves six layers (ABCACB ABCACB . . .). Similarly, in the 15R polytype the basic sequence involves fifteen layers (ABCACBCABACABCB . . .). The II–VI semiconductor, α-HgS, can also crystallize in the rhombohedral (red cinnabar) structure.

(c) Rocksalt structure

The II–VI compound MgO crystallizes in the rocksalt (NaCl) structure. The rocksalt structure shown in Figure 1.2(d) is typical of ionic bonding. The Bravais lattice is face-centered

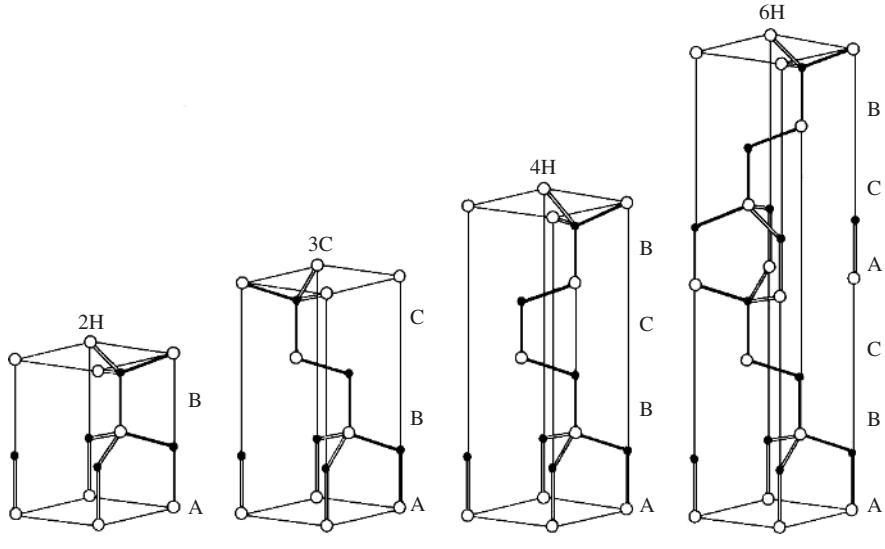

Figure 1.3 Three-dimensional perspective view of the 2H-SiC, 3C-SiC, 4H-SiC and 6H-SiC polytypes. The characteristic chain structures are represented by the heavy solid lines in the $(11\bar{2}0)$ plane. The stacking sequences AB (2H), ABC (3C), ABCB (4H) and ABCACB (6H) are also indicated. [From P. Käckell, B. Wenzien, and F. Bechstedt, *Phys. Rev. B* **50**, 17037 (1994), reproduced by permission from the American Physical Society]

cubic with the unit cell of atomic pattern consisting of one Mg and one O ion separated by one-half the body diagonal of the cube. Since each ion has six nearest neighbors of the opposite kind, the coordination number is six.

We summarize in Table 1.6 the crystal classes for easily or normally grown: (a) group-IV, (b) III–V and (c) II–VI binaries. Table 1.7 also lists the crystal structure for a number of group-IV, III–V and II–VI semiconductors.

1.3.2 Space group

A self-consistent arrangement of symmetry elements in a crystal lattice is known as a space group. The operation of any element of the group must have the pattern of symmetry elements unaltered. By inspection of the 230 space groups, or from first principles, there are just 32 different point groups. Crystals are, therefore, divided into 32 crystal classes according to the point-group symmetry they possess. In Table 1.7, we list the space (point) group for a number of group-IV, III–V and II–VI semiconductors.

Table 1.6 Summary of easily or normally grown crystal structure for: (a) group-IV; (b) III–V and; (c) II–VI semiconductors. d = diamond; zb = zinc-blende; h = hexagonal (wurtzite); rh = rhombohedral (trigonal); rs = rocksalt; or = orthorhombic

(a)

IV/IV	Si	C
Si	d	zb, h, rh
C	zb, h, rh	d

(b)

III/V	N	P	As	Sb
B	zb, h	zb	zb	
Al	h	zb	zb	zb
Ga	h	zb	zb	zb
In	h	zb	zb	zb

(c)

II/VI	O	S	Se	Te
Mg	rs	rs	zb	h
Zn	h	zb, h	zb	zb
Cd	rs	h	h	zb
Hg	rh, or	rh, zb	zb	zb

Table 1.7 Crystal structure, space group (point group) and lattice constants a and c ($T = 300$ K) for a number of group-IV, III–V and II–VI semiconductors. d = diamond; zb = zinc-blende; h = hexagonal; rh = rhombohedral; w = wurtzite; rs = rocksalt

System	Material	Crystal structure	Space group	a (Å)	c (Å)
IV	Diamond	d	$Fd3m$ (O_h)	3.5670	
	Si	d	$Fd3m$ (O_h)	5.4310	
	Ge	d	$Fd3m$ (O_h)	5.6579	
	α-Sn	d	$Fd3m$ (O_h)	6.4892	
	3C-SiC	zb	$F\bar{4}3m(T_d)$	4.3596	
	6H-SiC	h	$P6_3mc$ (C_{6v})	3.0806	15.1173
	15R-SiC	rh	$R3m$ (C_{3v})	3.079 ($\alpha = 13^\circ 54.5'$)	37.78
III–V	c-BN	zb	$F\bar{4}3m(T_d)$	3.6155	
	h-BN	h	$P6_3/mmc$ (D_{6h})	2.5040	6.6612
	BP	zb	$F\bar{4}3m(T_d)$	4.5383	
	BAs	zb	$F\bar{4}3m(T_d)$	4.777	
	w-AlN	w	$P6_3mc$ (C_{6v})	3.112	4.982
	c-AlN	zb	$F\bar{4}3m(T_d)$	4.38	
	AlP	zb	$F\bar{4}3m(T_d)$	5.4635	
	AlAs	zb	$F\bar{4}3m(T_d)$	5.66139	
	AlSb	zb	$F\bar{4}3m(T_d)$	6.1355	
	α-GaN	w	$P6_3mc$ (C_{6v})	3.1896	5.1855
	β-GaN	zb	$F\bar{4}3m(T_d)$	4.52	
	GaP	zb	$F\bar{4}3m(T_d)$	5.4508	
	GaAs	zb	$F\bar{4}3m(T_d)$	5.65330	
	GaSb	zb	$F\bar{4}3m(T_d)$	6.09593	
	InN	w	$P6_3mc$ (C_{6v})	3.548	5.760
	InP	zb	$F\bar{4}3m(T_d)$	5.8690	
	InAs	zb	$F\bar{4}3m(T_d)$	6.0583	
	InSb	zb	$F\bar{4}3m(T_d)$	6.47937	
II–VI	MgO	rs	$Fm3m(O_h)$	4.203	
	β-MgS	zb	$F\bar{4}3m(T_d)$	5.62	
	β-MgSe	zb	$F\bar{4}3m(T_d)$	5.91	
	β-MgTe	zb	$F\bar{4}3m(T_d)$	6.42	
	ZnO	w	$P6_3mc$ (C_{6v})	3.2495	5.2069
	α-ZnS	w	$P6_3mc$ (C_{6v})	3.8226	6.2605
	β-ZnS	zb	$F\bar{4}3m(T_d)$	5.4102	
	ZnSe	zb	$F\bar{4}3m(T_d)$	5.6692	
	ZnTe	zb	$F\bar{4}3m(T_d)$	6.009	
	c-CdS	zb	$F\bar{4}3m(T_d)$	5.825	
	w-CdS	w	$P6_3mc$ (C_{6v})	4.1367	6.7161
	c-CdSe	zb	$F\bar{4}3m(T_d)$	6.077	
	w-CdSe	w	$P6_3mc$ (C_{6v})	4.2999	7.0109
	CdTe	zb	$F\bar{4}3m(T_d)$	6.481	
	β-HgS	zb	$F\bar{4}3m(T_d)$	5.8514	
	HgSe	zb	$F\bar{4}3m(T_d)$	6.084	
	HgTe	zb	$F\bar{4}3m(T_d)$	6.4603	

1.4 LATTICE CONSTANT AND RELATED PARAMETERS

1.4.1 Lattice constant

(a) Room-temperature value

The lattice in the zinc-blende and rocksalt crystals can be defined by the one length parameter a. In hexagonal crystals, the lattice can be defined by the two length parameters, a and c. In rhombohedral crystals, the lattice can also be defined by the two length parameters, a and c, plus one angle parameter α. We have listed in Tables 1.4, 1.5 and 1.7 the lattice constants for a number of group-IV, III–V and II–VI semiconductors at $T = 300$ K. Figure 1.4 also plots the lattice constant a versus molecular weight $M = M_A + M_B$ for $A^N B^{8-N}$ semiconductors. From this plot, we can obtain the relation between a and M (a in Å; M in amu)

$$a = 0.579 + 1.04 \ln M \tag{1.8}$$

(b) Near-neighbor distance

There is a significant structural difference between the bond distance in the zinc-blende and wurtzite structures of binary compounds $A^N B^{8-N}$. The zinc-blende structure has only one type of first-neighbor distance

$$d(A - B) = \frac{\sqrt{3}}{4} a \text{ (four bonds)} \tag{1.9}$$

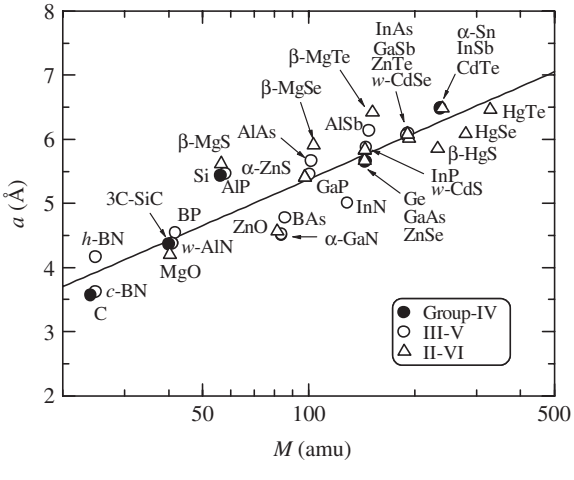

Figure 1.4 Lattice constant a versus molecular weight M for a number of group-IV, III–V and II–VI semiconductors. For hexagonal semiconductors, an effective lattice constant $a_{\text{eff}} = (\sqrt{3}a^2c)^{1/3}$ is plotted instead of a. The solid line represents the least-squares fit with $a = 0.579 + 1.04 \ln M$ (a in Å; M in amu)

Yet, the wurtzite structure has two types of first-neighbor anion–cation bond distances

$$d(\mathrm{A}-\mathrm{B}_1) = ua \text{ (one bond)} \tag{1.10a}$$

$$d(\mathrm{A}-\mathrm{B}_2) = \sqrt{\frac{1}{3} + \left(\frac{1}{2} - u\right)^2 \left(\frac{c}{a}\right)^2}\, a \text{ (three bonds)} \tag{1.10b}$$

where u denotes the cell internal structural parameter. In the case of an ideal tetragonal ratio $c/a = (8/3)^{1/2} = 1.633$ and an ideal cell internal parameter $u = 3/8$, it follows from Equation (1.10) that $d(\mathrm{A}-\mathrm{B}_1) = d(\mathrm{A}-\mathrm{B}_2)$.

In the case of the rocksalt structure, there is only one type of first-neighbor anion–cation bond distance

$$d(\mathrm{A}-\mathrm{B}) = \frac{a}{2} \quad \text{(six bonds)} \tag{1.11}$$

(c) External perturbation effect

The lattice constant is dependent to a great extent on both temperature and pressure. The temperature dependence of the lattice constant is explained by the thermal expansion coefficient. The lattice constant is related to the pressure by Murnaghan equation of state. It is also noted that the lattice constant is influenced by the crystalline perfection (i.e., stoichiometry, impurities, dislocations and surface damage). A well-known example is the dilation, or expansion, of the GaAs lattice induced by Te doping. Increase in the GaAs lattice constant of $\sim$0.01% has been reported at Te concentrations of $\sim 10^{19}$ cm^{-3} (see [1.7]).

1.4.2 Molecular and crystal densities

Molecular density d_{M} is given by

$$d_{\mathrm{M}} = \frac{8}{a^3} \tag{1.12}$$

for the diamond-type semiconductors,

$$d_{\mathrm{M}} = \frac{4}{a^3} \tag{1.13}$$

for the zinc-blende-type and rocksalt-type semiconductors and

$$d_{\mathrm{M}} = \frac{4}{a_{\mathrm{eff}}^3} \tag{1.14}$$

for the hexagonal (wurtzite) semiconductors, where a_{eff} is an effective cubic lattice constant defined by

$$a_{\mathrm{eff}} = (\sqrt{3}a^2 c)^{1/3} \tag{1.15}$$

The X-ray crystal density g can be simply written, in terms of d_M, as

$$g = \frac{M d_M}{N_A} \tag{1.16}$$

where M is the molecular weight and $N_A = 6.022 \times 10^{23}$ mol^{-1} is the Avogadro constant. We have listed in Tables 1.4 and 1.5 the values of g for a number of group-IV, III–V and II–VI semiconductors with cubic and hexagonal structures, respectively.

1.5 STRUCTURAL PHASE TRANSITIONS

It is known that at high pressure the group-IV elemental semiconductors show metallic transitions in a sequence from cubic (diamond)→tetragonal (β-Sn)→simple hexagonal→ hexagonal close packed. Similarly, the III–V and II–VI semiconductors exhibit a variety of the crystal structures at high pressures. In Table 1.6, we have summarized the crystal classes for easily or normally grown group-IV, III–V and II–VI binary semiconductors.

The electrical resistivity of semiconductors is known to drop discontinuously by several orders of magnitude at the transition pressures; therefore the phase transitions have been studied chiefly by electrical measurements. There have also been some attempts to determine the crystalline structures of the high-pressure polymorphs of semiconductors by various techniques, such as X-ray diffraction, optical microscopy and Raman scattering [1.8].

It is interesting to note the correlations between the ambient properties and high-pressure behavior. Chelikowsky [1.9] discussed empirical scales for transition pressures as a function of ionicity and bond length. By fixing his scaling parameters by experiment and theory, it becomes possible to determine the transition pressures for the zinc-blende to β-Sn structure and for the zinc-blende to rocksalt transition.

Table 1.8 Transition pressure to the first phase P_T for some group-IV, III–V and II–VI semiconductors

System	Material	P_T (GPa)	System	Material	P_T (GPa)
IV	Si	12	II–VI	ZnO	8.0–10
	Ge	12		α-ZnS	10.7–11.4
				β-ZnS	14.7–17.4
III–V	w-AlN	14–22.9		ZnSe	11.8–14.6
	AlP	9.5–17.0		ZnTe	7 –9.5
	AlAs	7–14.2		w-CdS	1.75–3
	AlSb	5.3–12.5		w-CdSe	2.13–2.9
	α-GaN	37–53.6		CdTe	3.53
	GaP	21.5		HgSe	0.7–0.75
	GaAs	16.6–17.3		HgTe	1.4
	GaSb	6.2–7.0			
	InN	12.1–23.0			
	InP	10.8			
	InAs	7			
	InSb	2.2			

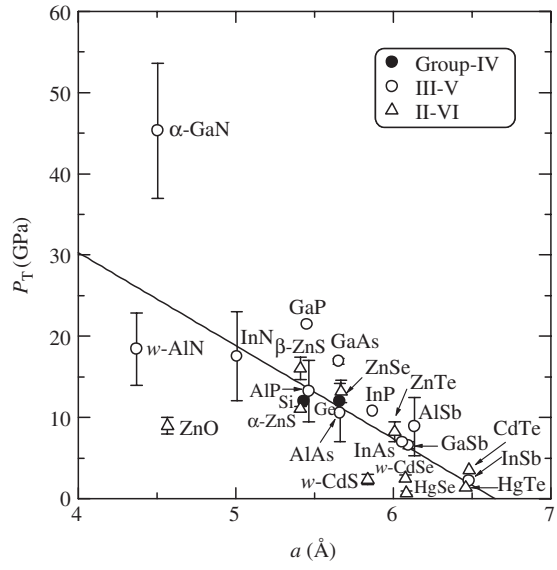

Figure 1.5 Transition pressure to the first phase P_T versus lattice constant a for some group-IV, III–V and II–VI semiconductors. For hexagonal semiconductors, an effective lattice constant $a_{eff} = (\sqrt{3}a^2c)^{1/3}$ is plotted instead of a. The solid line represents the least-squares fit with $P_T = 76.2 - 11.5a$ (a in Å; P_T in GPa)

We list in Table 1.8 the transition pressure to the first phase P_T observed for some group-IV, III–V and II–VI semiconductors. Figure 1.5 also plots P_T versus lattice constant a for these semiconductors. The solid line represents the least-squares fit with the relation (a in Å; P_T in GPa)

$$P_T = 76.2 - 11.5a \tag{1.17}$$

We summarize in Table 1.9 the sequence of the structural phase transitions for a number of group-IV, III–V and II–VI semiconductors observed at high pressures.

1.6 CLEAVAGE

1.6.1 Cleavage plane

The cleavage properties of a crystal are strongly related to the atomic arrangement and corresponding electron density map. The principles that determine a plane of cleavage are as follows:

1. The number of 'bonds' (nearest neighbors) to be separated per unit area of the plane is a minimum, as compared with all other crystal planes.
2. The plane is electrically neutral, with alternate arrays of positive and negative structure elements which permit the two separating surface layers to assume repelling positions when shifted with respect to each other.

Table 1.9 Sequence of the structural phase transitions observed for a number of group-IV, III–V and II–VI semiconductors at high pressures. bcc = body-centered cubic; bct = body-centered tetragonal; cin = cinnabar; d = diamond; dCsCl = distorted CsCl; dhc = double hexagonal close-packed; fcc = face-centered cubic; h = hexagonal; hcp = hexagonal close-packed; or = orthorhombic; rh = rhombohedral; rs = rocksalt (NaCl); sh = simple (primitive) hexagonal; w = wurtzite; zb = zinc-blende

System	Material	Crystal structure (normal pressure→high pressure)
IV	Diamond	d→no phase transition up to experimentally available pressure
	Si	d→ β-Sn→or (*Imma*)→sh→or (*Cmca*)→hcp→fcc
	Ge	d→ β-Sn→or (*Imma*)→sh→dhc (d→ β-Sn→or (*Imma*)→sh→or (*Cmca*)→hcp)
	α-Sn	d→(β-Sn)→bcc
	3C-SiC	zb→rs
	6H-SiC	h→rs
	15R-SiC	rh→no phase transition up to 150 GPa
III–V	*c*-BN	zb→no phase transition up to 115 GPa
	h-BN	h→?
	BP	zb→no phase transition up to 68 GPa
	BAs	zb→?
	w-AlN	w→rs
	c-AlN	zb→?
	AlP	zb→ β-Sn/h (NiAs)
	AlAs	zb→h (NiAs)
	AlSb	zb→ β-Sn/rs/or→unknown
	α-GaN	w→rs
	β-GaN	zb→?
	GaP	zb→ β-Sn
	GaAs	zb→or (*Pmm*2)/or (*Cmcm*)→or (*Imm*2)→sh
	GaSb	zb→ β-Sn/or (*Imma*)→sh→unknown
	InN	w→rs
	InP	zb→rs→ β-Sn/or (*Cmcm*)
	InAs	zb→rs→ β-Sn/or (*Cmcm*)
	InSb	zb→ β-Sn (?)→or (*Immm*)→or (*super-Cmcm*)→(?)→bcc (?)
II–VI	MgO	rs→no phase transition up to 227 GPa
	β-MgS	zb→?
	β-MgSe	zb→?
	β-MgTe	zb→?
	ZnO	wz→rs
	α-ZnS	wz→zb→rs
	β-ZnS	zb→rs→or (*Cmcm*)
	ZnSe	zb→rs→sh
	ZnTe	zb→cin→or (*Cmcm*)
	c-CdS	zb→wz (high temperature)
	w-CdS	wz→rs→or (*Pmmn*)
	c-CdSe	zb→wz (high temperature)
	w-CdSe	wz→rs
	CdTe	zb→cin→rs→or (*Cmcm*)
	β-HgS	zb→cin
	HgSe	zb→cin→rs→bct
	HgTe	zb→cin→rs→or (*Cmcm*)→dCsCl

Figure 1.6 represents schematic views of the atomic rearrangement in the direction along the (110), (111) and (100) planes of the zinc-blende lattice (GaAs). This arrangement is the same as for the diamond lattice, except that the two different kinds of atom occupy alternate positions in the lattice. Table 1.10 summarizes the crystallographic plane most readily cleaved for the diamond, zinc-blende, wurtzite and rocksalt structures.

In diamond-type crystals, such as diamond and Si, cleavage occurs along (111) surface planes. This is because the (111) surface atoms are only singly bonded to the opposite surface, but the (100) surface atoms are doubly bonded to the opposite surface (see Figure 1.6). The (110) surface atoms are also singly bonded to the opposite surface, but the plane spacing is shorter than that of the (111) planes. It is more difficult to separate the planes of shorter spacing.

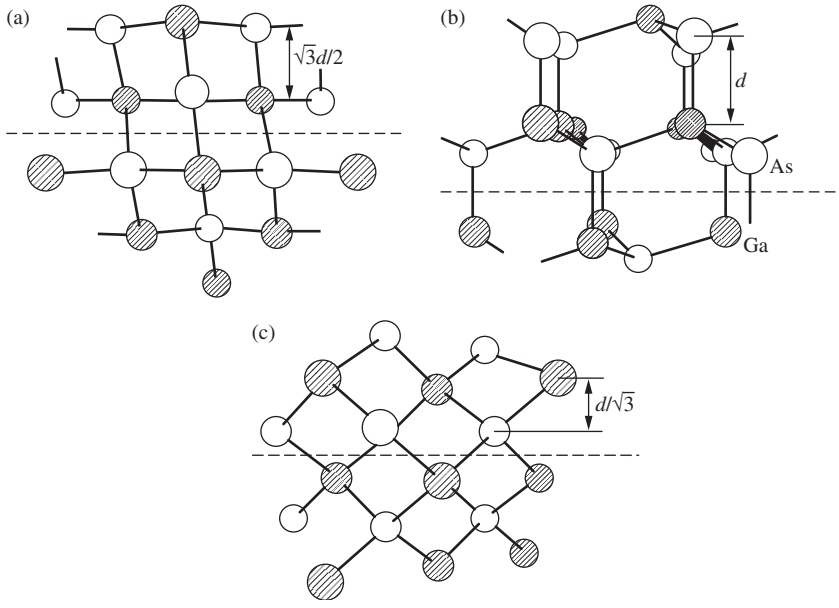

Figure 1.6 Schematic views of the atomic arrangement in the direction along the (110) (a), (111) (b) and (100) planes (c) of GaAs. Note that this arrangement is the same as the diamond lattice, except that the two different kinds of atom (Ga, As) occupy alternate positions in the lattice. The principal cleavage in the zinc-blende crystals is in a plane parallel to (110) (a), and that in the diamond-type crystals is in a plane parallel to (111) (b)

Table 1.10 Crystallographic plane most readily cleaved for various crystal structures

Crystal structure	Cleavage plane
Diamond	(111)
Zinc-blende	(110)
Wurtzite	$(11\bar{2}0)$, $(10\bar{1}0)$
Rocksalt	(100)

In the case of zinc-blende-type lattice, we must take into account the effects of surface polarity and electron density distribution. The zinc-blende-type lattice has two types of (111) surface polarities, (111)A and (111)B, and hence there will be an electrostatic attraction between these different planes. Such an attractive force will make it difficult to separate along the (111) planes. However, the (110) surfaces are composed of equal numbers of A and B atoms, so there will be no overall electrostatic force between the planes. Wolff and Broder [1.10] have investigated the bonding character and microcleavage in materials with tetrahedral coordination. They found that the (110) plane is the principal cleavage plane in III–V compounds. They also found microcleavages in GaAs in (*hhk*) planes ($h \geqslant k$). The microcleavage is revealed by the observation of light figure patterns from cleavage pits produced by grinding or abrading the surface.

The surface energy $E\gamma$ is defined by energy per unit surface area necessary to separate a crystal along a given plane. Berding *et al.* [1.11] have calculated the cleavage energies $E\gamma$ for Si, GaAs, CdTe and HgTe. Their results give an ordering of $E\gamma$(Si)> $E\gamma$(GaAs)> $E\gamma$(CdTe)> $E\gamma$(HgTe) for the experimentally observed cleavage planes; i.e., for the cleavage on (111) in Si and (110) in GaAs, CdTe and HgTe. This ordering is what one would expect based on simple bond-length and bond-density arguments. A simple estimate of the cleavage energy can be made by multiplying the number of bonds broken per unit area on the cleavage surfaces by the energy per bond. Thus, although for a given bond-length, the bond-density on the (110) surface (on which GaAs cleaves) is higher than on the (111) surface (on which Si cleaves), the shorter bond-length and the larger bond-strength of Si compared with GaAs combine to produce a larger cleavage energy in Si. In turn, both the shorter bond-length and the larger bond-strength of GaAs compared with HgTe and CdTe result in a larger cleavage energy in GaAs. Finally, the weaker HgTe bond, compared with CdTe, and their nearly equal bond lengths predict a smaller cleavage energy in HgTe.

It has been shown experimentally [1.12] that the (112) cleavage planes can be obtained, as the secondary cleavage plane, in the twinned regions between the (110) cleavage surfaces of the matrix grains in CdTe. Like the (111) surfaces, the (112) surfaces in the zinc-blende crystals have surface polarity. The electrostatic attraction in highly ionic II–VI compounds should contribute considerably to the cleavage energy for the (112) surfaces. This consideration predicts that the (112) surfaces may be more easily cleaved in III–V compounds than in II–VI compounds.

On the basis of the above-mentioned principle, it is possible to verify the $(11\bar{2}0)$ (and/or $(10\bar{1}0)$) and (100) planes as the most readily cleaved planes for the wurtzite (hexagonal) and rocksalt structures, respectively.

1.6.2 Surface energy

(a) Theoretical value

In an attempt to explain the 'easy' cleavage of solids, various methods have been employed to calculate the energies required to cleavage a crystal parallel to a particular plane. The cleavage energy was assumed equal to twice the surface energy of that plane. In this approximate method, the surface energy is calculated as the number of bonds cut per unit area multiplied by the thermodynamic energy of each bond, irrespective of whether

Table 1.11 Theoretical surface (cleavage) energy for some planes of cubic group-IV, III–V and II–VI semiconductors (J/m^2)

System	Material	(100)	(110)	(111)	$(\bar{1}\bar{1}\bar{1})$
IV	Diamond	9.2	6.5	5.3	
	Si	1.99	1.41	1.15	
	Ge			0.88–1.00	
	α-Sn			0.662	
	3C-SiC	1.908–4.65	2.330	1.767	0.7184
III–V	*c*-BN		4.53	4.02	3.07
	BP		2.38	1.64	1.93
	BAs		2.06	1.39	1.88
	c-AlN		2.12	2.30	1.12
	AlP		1.37	1.19	0.956
	AlAs		1.21	1.01	0.935
	AlSb		1.050	0.814	0.945
	GaP		1.38	1.24	0.95
	GaAs	1.06	1.00	1.05	
	GaSb		0.995	0.803	0.900
	InP		1.08	1.09	0.80
	InAs		1.015	0.980	0.728
	InSb		0.814	0.738	0.690
II–VI	β-ZnS		1.225	1.15	0.85
	ZnSe		0.98	0.885	0.75
	ZnTe		0.96	0.808	0.84
	c-CdS		1.06	1.07	0.69
	c-CdSe		0.94	0.91	0.88
	CdTe	0.85	0.18	0.58	
	β-HgS		1.13	1.00	0.73
	HgTe	0.05	0.12	0.09	

Table 1.12 Theoretical surface (cleavage) energy for some planes of hexagonal group-IV and II–VI semiconductors (J/m^2)

System	Material	(0001)	$(000\bar{1})$
IV	6H-SiC	1.80[a]	0.75[a]
II–VI	ZnO	1.95	0.96
	α-ZnS	1.30	0.96

[a] 4H-SiC value

Table 1.13 Cleavage plane and experimental surface energy for some group-IV, III–V and II–VI semiconductors. The experimental data are taken from various sources

System	Material	Crystal structure	Cleavage plane	Surface energy (J/m^2)
IV	Si	Diamond	(111)	1.14–1.240
	Ge	Diamond	(111)	1.060
III–V	GaP	Zinc-blende	(110)	1.96
	GaAs	Zinc-blende	(110)	0.86
II–VI	MgO	Rocksalt	(100)	1.2

the 'cut' is at an angle to the bonding direction. We summarize in Tables 1.11 and 1.12 the theoretical surface energies for some cubic and hexagonal semiconductors, respectively [1.11, 1.13–1.17].

Berding *et al*. [1.11] have presented a method for the calculation of the surface energy $E\gamma$ for Si based on a tight-binding Green's function approach, and obtained that $E\gamma$ for the (111) surface is considerably smaller than those for the (100) and (110) surfaces. The same conclusion has also been obtained by Hesketh *et al*. [1.14]

(b) Experimental value

There is a dearth of experimental measurements of surface energy. This is because many difficulties are associated with measuring it; especially when indirect methods are used. Since the surface energy can be defined as the work that is required to separate a crystal into two parts along a plane, cleavage is a particularly direct way of measuring it [1.18]. We list in Table 1.13 the experimentally determined surface energies for some group-IV, III–V and II–VI semiconductors.

REFERENCES

[1.1] J. C. Phillips, *Bonds and Bands in Semiconductors* (Academic, New York, 1973).
[1.2] See, J. C. Phillips, *Rev. Mod. Phys.* **42**, 317 (1970).
[1.3] W. A. Harrison, *Phys. Rev. B* **8**, 4487 (1973).
[1.4] D. R. Lide, *CRC Handbook of Chemistry and Physics*, 78th Edition (CRC Press, Boca Raton, 1997).
[1.5] A. R. Verma and P. Krishna, *Polymorphism and Polytypism in Crystals* (Wiley, New York, 1966).
[1.6] P. Käckell, B. Wenzien, and F. Bechstedt, *Phys. Rev. B* **50**, 17037 (1994).
[1.7] S. Adachi, *GaAs and Related Materials: Bulk Semiconducting and Superlattice Properties* (World Scientific, Singapore, 1994).
[1.8] U. D. Venkateswaran, L. J. Cui, B. A. Weinstein, and F. A. Chambers, *Phys. Rev. B* **45**, 9237 (1992), and references cited therein.
[1.9] J. R. Chelikowsky, *Phys. Rev. B* **35**, 1174 (1987).
[1.10] G. A. Wolff and J. D. Broder, *Acta Cryst.* **12**, 313 (1959).
[1.11] M. A. Berding, S. Krishnamurthy, A. Sher, and A.-B. Chen, *J. Appl. Phys.* **67**, 6175 (1990).

[1.12] H. Iwanaga, A. Tomizuka, and T. Shoji, *J. Mater. Sci. Lett.* **10**, 975 (1991).
[1.13] J. E. Field, in *Properties and Growth of Diamond*, EMIS Datareviews Series No. 9, edited by G. Davies (INSPEC, London, 1994), p. 36.
[1.14] P. J. Hesketh, C. Ju, S. Gowda, E. Zanoria, and S. Danyluk, *J. Electrochem. Soc.* **140**, 1080 (1993).
[1.15] B. N. Oshcherin, *Phys. Status Solidi A* **34**, K181 (1976).
[1.16] T. Takai, T. Halicioğlu, and W. A. Tiller, *Surf. Sci.* **164**, 341 (1985).
[1.17] R. Yakimova, M. Syväjärvi, and E. Janzén, *Mater. Sci. For.* **264–268**, 159 (1998).
[1.18] J. J. Cilman, *J. Appl. Phys.* **31**, 2208 (1960).